DOI: 10.1002/adem.201500389

An Assessment of the Role of Fiber Coating and Suspending Fluid on the Deposition of Carbon Nanotubes onto Glass Fibers for Multiscale Composites**

By *J. J. Ku-Herrera, A. May-Pat* and *F. Avilés**

Multiwall carbon nanotubes (MWCNTs) were ultrasonically deposited onto glass fibers by using either distilled water or a hydrolyzed silane. The role of the fiber coating (sizing) was investigated by depositing MWCNTs onto glass fibers with and without sizing. The interfacial shear strength (IFSS) between the MWCNT-modified fibers and a vinyl ester matrix was analyzed by the microbond test. Increased electrical conductivity and surface roughness was achieved upon MWCNT deposition on the fibers. The use of a silane as suspending fluid renders moderate benefits with respect to distilled water, and its role is more critical in improving the IFSS between the MWCNT-modified fibers and the matrix.

1. Introduction

The recent advances of nanotechnology and the commercial availability of nanoscale materials have motivated the development of multiscale hierarchical composites with multifunctional properties. In particular, the outstanding mechanical,[1] electrical,[2] and thermal[3] properties of carbon nanotubes (CNTs) in combination with their high aspect ratio (length/diameter) and low density[4] make them ideal candidates to develop hierarchical composites with multifunctional properties. Many research works have incorporated CNTs in hierarchical composites either by placing them within the polymer matrix[5] or onto micron-size fibers.[6] When the CNTs are randomly incorporated into the polymer matrix, given their high aspect ratio and surface area, they may form agglomerates which act as stress concentrators deteriorating the mechanical properties of the composite.[6b,7] An alternative for damage sensing applications based on electrical resistance consists in placing the CNTs directly onto the fiber's surface. Some methods to achieve this aim imply direct growth of CNTs on the fibers[8] or wet procedures by simply dipping[9] or assisted by electric fields.[9,10] Synthesizing CNTs directly onto engineering fibers can detriment the fiber strength due to thermal degradation of the fibers.[8a,11] Besides, such processes can be more difficult to scale up than the ones based on wet deposition. Thus, dip-coating deposition has arisen as a simple and attractive manufacturing procedure to place CNTs onto micron-size fibers, aiming towards the development of multiscale hierarchical composites. In spite of the advances in this field, more research efforts need to be conducted in order to homogeneously place a high-density of electrically percolating CNTs onto the fibers. Additionally, since placing CNTs onto structural fibers implies the modification of the fiber/matrix interface,[8a,12] more research efforts need to be devoted to increase the understanding of the mechanisms of interaction between the MWCNT-modified fibers and the matrix. Given this motivation, the present work investigates the deposition of multiwall CNTs (MWCNTs) onto commercial glass fibers, focusing on the role of silane and water as the deposition mediums and the concomitant role of the silane as coupling agent between the MWCNT/glass fibers and a vinyl ester resin. The issue of removing the coating ("sizing") or not from the glass fibers before MWCNT deposition is also addressed. Scanning electron microscopy (SEM) and Raman spectroscopy are employed to examine the dispersion and distribution of MWCNTs onto the glass fibers. The surface roughness of the fibers covered with MWCNTs is analyzed by atomic force microscopy. The electrical conductivity of such glass fibers upon MWCNT deposition is a key feature to render strain and damage sensing capabilities to these kind of hierarchical composites, and therefore is also investigated. Additionally, the role of the silane on the interfacial shear

---

[*] *Dr. F. Avilés, Dr. J. J. Ku-Herrera, Dr. A. May-Pat*
Centro de Investigación Científica de Yucatán A.C., Unidad de Materiales, Calle 43 No.130, Col. Chuburná de Hidalgo. C.P. 97200, Mérida, Yucatán, Mexico
E-mail: faviles@cicy.mx

[**] *This work was supported by CONACYT project number 220513 under the direction of Dr. Avilés. Technical support of Javier Cauich and Santiago Duarte from CICY is appreciated.*

strength (IFSS) between the modified glass fibers and a vinyl ester polymer matrix is analyzed by the microbond test.

2. Materials and Methods

2.1. Materials

Commercial E-glass fibers (Poliformas Plásticas S.A de C.V. Mérida, Mexico) with an average diameter of 15 μm, density of 2.54 g cm^{-3} in the form of fiber tows (≈4 000 filaments per tow) were used. The glass fibers were used as-received (containing a fiber coating or "sizing") as well as after removing their proprietary coating by Soxhlet extraction in acetone. Commercial MWCNTs (Cheap Tubes Inc., Vermont, USA) with purity >95%, 30–50 nm outer diameter, 5–10 nm inner diameter, and 1–6 μm length were used. The MWCNTs were chemically oxidized using a solution of H_2SO_4/HNO_3 at 3.0 M for 2 h, following the procedure reported in ref.[13] This procedure generates hydroxyl and carboxyl functional groups on the MWCNT surface.[13] The MWCNTs were deposited onto the glass fibers using either distilled water as suspending/deposition medium or a mixture of water/silane. The silane coupling agent employed was 3-(trimethoxysilyl) propyl methacrylate (MPS, Sigma–Aldrich, St. Louis, Missouri, USA), which has proven to act as an efficient coupling agent between the oxidized MWCNTs and the vinyl ester resin.[14] A Derakane Momentum 470–300 resin (Ashland performance materials, Dublin, Ohio, USA) was used for the characterization of the IFSS using the microdrop test. Methyl ethyl ketone (initiator) and cobalt naphthenate (promoter) both at 0.5 wt% (with respect to the resin weight) were used to polymerize the vinyl ester.

2.2. Deposition of MWCNTs onto Glass Fibers

Two groups of fibers were employed for the deposition of MWCNTs. The first group of fibers were used as received (CC, for "coating-containing") and a second group of fibers had the coating removed (CR, for "coating-removed"). For CR fibers, the coating (sizing) was removed by conventional Soxhlet extraction in acetone. For both groups of fibers the MWCNTs were deposited onto the glass fibers using one of the following suspending fluids: i) distilled water (W), or ii) a hydrolyzed silane (Si), see Table 1. In such a table, the first letter of the identification label refers to the deposition medium (W or Si) and the other two letters indicate if the glass fibers were employed with (CC) or without (CR) coating.

Table 1. Identification of conditions used to deposit MWCNTs onto the glass fibers.

MWCNTs' suspending fluid	Glass fiber condition	Identification
Water (W)	Coating removed (CR)	W-CR
	Coating containing (CC)	W-CC
Hydrolyzed silane (Si)	Coating removed (CR)	Si-CR
	Coating containing (CC)	Si-CC

Upon MWCNT deposition onto glass fibers, such MWCNT-modified fibers are expected to interact with the polymer matrix forming multiscale hierarchical composites with one of the four architectures schematized in Figure 1.

The deposition of MWCNTs onto the glass fibers was conducted following the procedure reported in ref.[15] Briefly, 5 mg of MWCNTs were added into 40 ml of water and dispersed for 2 h using an ultrasonic bath operated at 42 kHz and 70 W. The glass fibers (1 g) were immersed in the MWCNT/water solution and such a mixture was further dispersed in the ultrasonic bath for 3 h. Since MWCNTs are dispersed by ultrasonic forces, this procedure yields MWCNT infiltration among the micron-sized fibers, promoting physicochemical interactions among them such as van der Waal forces and hydrogen bonding. Finally, the glass fibers with deposited MWCNTs were removed from the container and dried in a convection oven at 100 °C overnight. For the second variation of the process, hydrolyzed MPS was used as the suspending fluid (deposition medium). For this variation, 5 mg of MWCNTs were added into 40 ml of distilled water and then dispersed using an ultrasonic bath for 1.5 h. Acetic acid was then added to the MWCNT/water mixture to obtain a pH of 5 and 5 wt% of MPS (with respect to the glass fiber weight) was added to the mixture, keeping such a mixture under ultrasonic agitation for 30 min to hydrolyze the silane. The glass fibers were then immersed into the hydrolyzed MPS solution and such a mixture was ultrasonically agitated for 3 h to deposit the MWCNTs onto the fibers. The MWCNT-modified fibers were then dried as explained above. Notice that the deposition time is the same using either water or hydrolyzed MPS.

2.3. Dispersion and Distribution of the Deposited MWCNTs onto the Glass Fibers

Scanning electron microscopy (SEM) and Raman spectroscopy were used to analyze the dispersion and distribution of

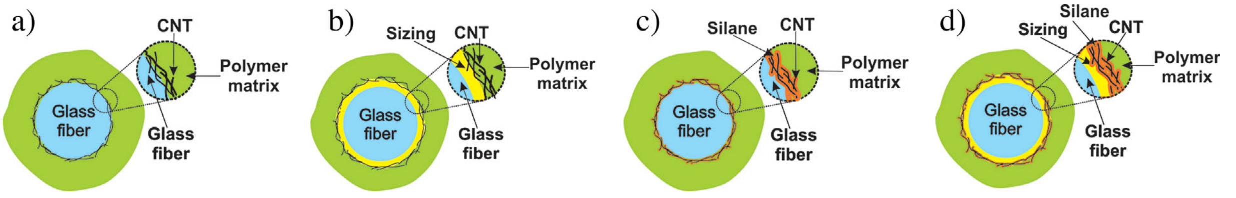

Fig. 1. Representation of the fiber/matrix interfacial region expected for the multiscale hierarchical architectures listed in Table 1. (a) W-CR, (b) W-CC, (c) Si-CR, and (d) Si-CC.

the MWCNTs deposited onto the glass fibers. The SEM characterization was conducted over randomly selected fiber tows using a JEOL JSM-6360LV SEM. For the Raman analysis, a dispersive micro-Raman equipped with a HeNe laser with a wavelength of 632.8 nm was used. Twenty Raman spectra for each fiber condition were obtained by collecting one Raman spectrum every 500 μm along the fiber, mapping the fiber length. The analysis was conducted on single fibers containing the deposited MWCNTs using an objective lens of 50×, during 30 s of exposure time and 5 accumulations. Raman spectra of the MWCNTs over the glass fiber as a function of the position on the fiber were obtained in this way.

2.4. Electrical Resistance of Individual Glass Fibers and Fiber Tows with Deposited MWCNTs

The electrical resistance (R) of individual glass fibers with deposited MWCNTs was measured as a function of the distance between electrodes using a two-point configuration. Three sets of fibers were cut to a total length of 10 mm, and then 2 mm long electrodes made of silver paint were instrumented onto the single fibers to define an effective electrode separation of 1, 3, or 5 mm. A Keithley 6517B electrometer was employed using 10 replicates for each electrode separation and condition. Additionally, the electrical resistance of tows composed of ≈4 000 glass fibers with deposited MWCNTs was also characterized. For this experiment, the tows were 40 mm long and 10 mm long electrodes were defined at the tow ends leaving an effective length of 20 mm.

2.5. Surface Roughness

The surface roughness of the glass fibers without and with MWCNTs was characterized by atomic force microscopy (AFM) using a Bruker SPM8 AFM in tapping mode. AFM analysis was conducted over a $3 \times 3\,\mu m^2$ sampled area. A statistical analysis of a central $2.5 \times 2.5\,\mu m^2$ section of the AFM sampled area was then carried out. The $2.5 \times 2.5\,\mu m^2$ area was divided into 25 sub-areas of $500 \times 500\,nm^2$ as depicted in Figure 2 and the root mean square (RMS) roughness of such sub-areas was measured using the "NanoScope Analysis" AFM software. Using the RMS roughness of each sub-area as a central metric, the average and coefficient of variation (CV) of the 25 data were calculated.

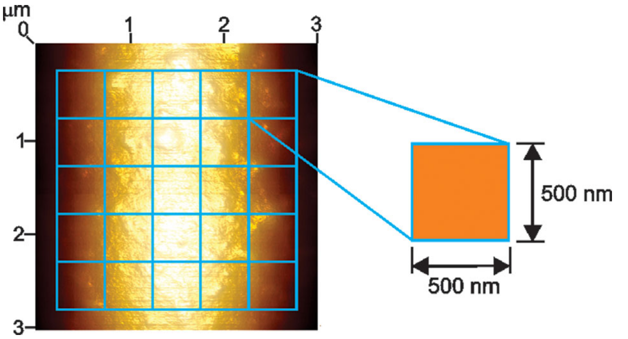

Fig. 2. Schematic of the AFM roughness analysis on the glass fiber.

2.6. Interfacial Shear Strength between a Glass Fiber and Vinyl Ester Resin

The interfacial shear strength (IFSS) between an individual glass fiber and the vinyl ester (VE) resin was analyzed by the microbond test. Microbond samples were prepared by fixing individual glass fibers into an aluminum frame, and placing small drops of the vinyl ester resin onto the fiber using a 3 mm diameter syringe. Twenty specimens with droplet embedded lengths (L_e) ranging from 60 to 170 μm were tested; larger resin droplets may induce fiber failure instead of interface failure as well as a non-axisymmetric droplet shape, and thus were discarded. The fiber diameter (d_f) and the embedded length were measured using an optical microscope prior testing. A constant displacement rate of $20\,\mu m\,min^{-1}$ and a 2.5 N load cell were used, and the applied axial force (P) was recorded up to droplet debonding.

The interfacial shear strength between the glass fiber and the VE resin was calculated according to the conventional debonding equation, which is based on the assumption of a constant IFSS between the fiber and its surrounding matrix,[16] i.e.,

$$\mathrm{IFFSS} = \frac{P_{\max}}{\pi d_f L_e} = \frac{m}{\pi d_f} \tag{1}$$

where $P_{\max}$ is the maximum force recorded at the onset of microdrop debonding and $\pi d_f L_e$ is the embedded area. Drop debonding at $P_{\max}$ was verified by optical microscopy and the slope of the plot of $P_{\max}$ versus L_e (m) was used in Equation 1 to calculate the IFSS.

3. Results and Discussion

3.1. Distribution of MWCNTs onto the Glass Fibers

Figure 3 shows the photographs and SEM images of the glass fibers containing MWCNTs which were deposited using distilled water and a hydrolyzed silane. Figure 3a and b are representative of the results of the procedure that used water as the suspending fluid to deposit MWCNTs onto fibers whose coating was previously removed (Figure 3a) or not (Figure 3b). Likewise, Figures 3c and d are representative of the results of the procedure that used a hydrolyzed silane as suspending fluid to deposit MWCNTs onto fibers whose coating was removed (Figure 3c) or not (Figure 3d).

In Figure 3a (left), the macroscale photograph of a tow of W-CR fibers shows some light gray regions as well as some darker regions indicating a nonhomogeneous deposition of MWCNTs onto these fibers. The non-homogeneous deposition of MWCNTs for W-CR fibers is confirmed by the aggregates seen in the SEM images of Figure 3a (center and right). However, for the same suspending fluid (water) when the glass fibers maintained their original coating, the W-CC fibers show a homogeneous black color at the macroscale

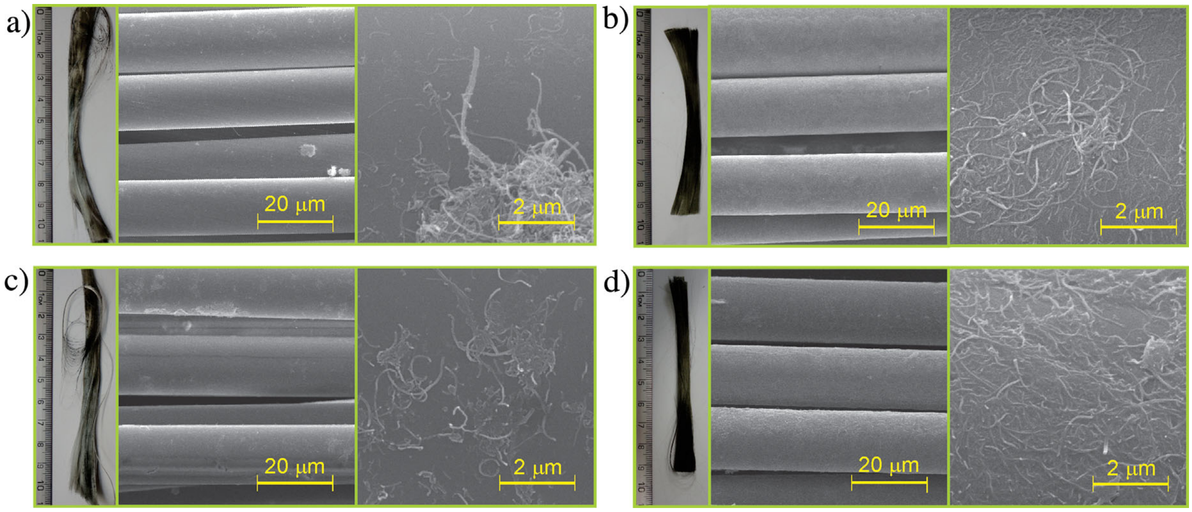

Fig. 3. Photographs and SEM images of deposited MWCNTs onto glass fibers. (a) W-CR, (b) W-CC, (c) Si-CR, and (d) Si-CC. Labels correspond to Table 1.

(Figure 3b, left) and the homogeneous deposit of MWCNTs is confirmed by the SEM images (Figure 3b center and right). Therefore, it is clear that the presence of the original fiber coating ("sizing") improves the interaction between the oxidized MWCNTs and the glass fibers, rendering a more homogeneous distribution. A similar situation is observed for the glass fibers whose MWCNT deposition used MPS. When a mixture of MPS/distilled water is used to deposit MWCNTs

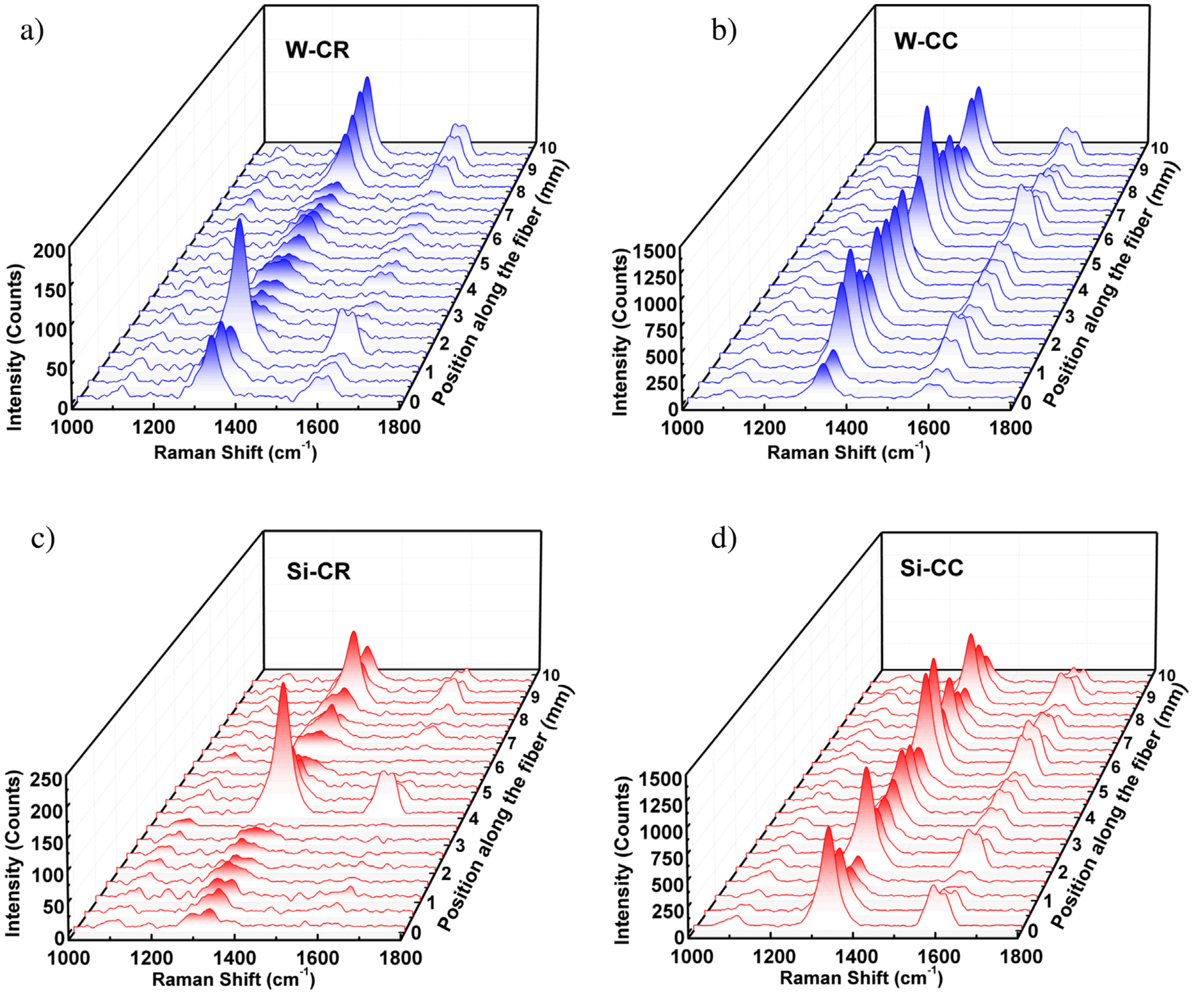

Fig. 4. Spatial maps constructed from the Raman spectra of glass fibers with deposited MWCNTs. (a) W-CR, (b) W-CC, (c) Si-CR, (d) Si-CC.

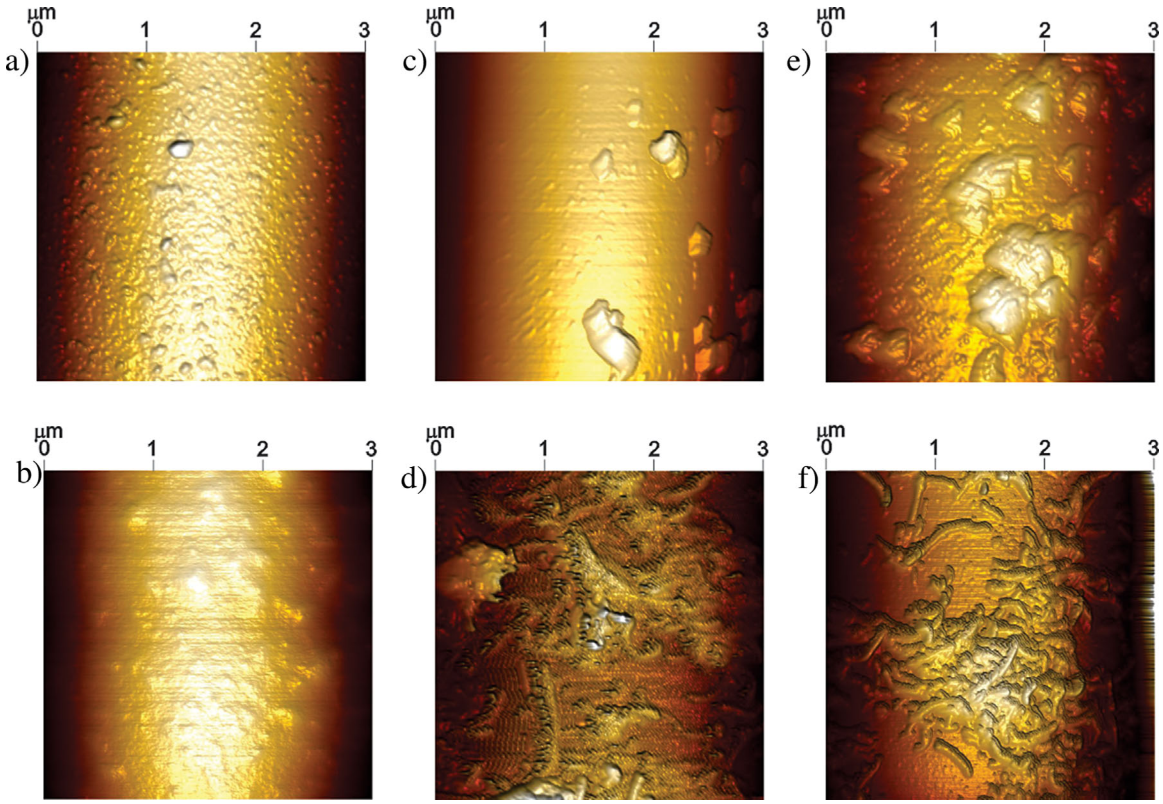

Fig. 5. AFM images of the glass fibers without and with MWCNTs. (a) CR, (b) CC, (c) W-CR, (d) W-CC, (e) Si-CR, and (f) Si-CC.

onto CR fibers, a non-uniform coverage of MWCNTs onto the glass fibers is observed (Figure 3c). On the other hand, using an identical process but for as-received glass fiber renders a relative uniform distribution and high density of MWCNTs, Figure 3d. Thus, a uniform deposition of MWCNTs onto the glass fibers is achieved only when the original fiber coating is maintained. It has been observed that the hydroxyl and carboxyl functional groups of the oxidized MWCNTs chemically interact with the hydroxyl and carbonyl groups of the fiber coating forming hydrogen bonding as well as through a ring opening reaction of the epoxy groups of the fiber coating.[15]

Raman spectroscopy was also exploited to further investigate the spatial distribution and density of MWCNTs on the fiber. The use of Raman spectroscopy to such an aim relies on the fact that the glass fibers do not present Raman features in the region where the MWCNTs show their stronger Raman features (1 100–1 800 cm^{-1}). [15] Therefore, the Raman signal of the glass fibers containing MWCNTs is associated solely to the presence of MWCNTs.

The Raman spectrum as a function of the position on the fiber is presented as a three-dimensional map in Figure 4. By comparing the distribution of the G (≈1 585) or D (≈1 330) band intensities along the fiber for W-CR (Figure 4a) and W-CC (Figure 4b), a higher intensity (≈10×) of the G band for W-CC fibers with respect to that of W-CR fibers is evident. Moreover, the significantly more homogeneous distribution of the G band intensities for W-CC with respect to W-CR, is interpreted as a clear signal of a more homogeneous deposition for W-CC. For Si-CR (Figure 4c), the distribution of the G band intensity along the fiber is again non-homogeneous and even vanishes at some regions (suggesting absence of MWCNTs at such regions). For Si-CC (Figure 4d) the magnitude and distribution of the G band intensities is

Table 2. RMS surface roughness (nm) of glass fibers with and without MWCNTs.

	Fiber condition					
	Without MWCNTs		With deposited MWCNTs			
Statistical parameter	CC	CR	W-CR	W-CC	Si-CR	Si-CC
RMS	2.07	4.05	6.26	26.7	8.86	17.8
CV	0.37	0.33	0.71	0.23	0.52	0.24

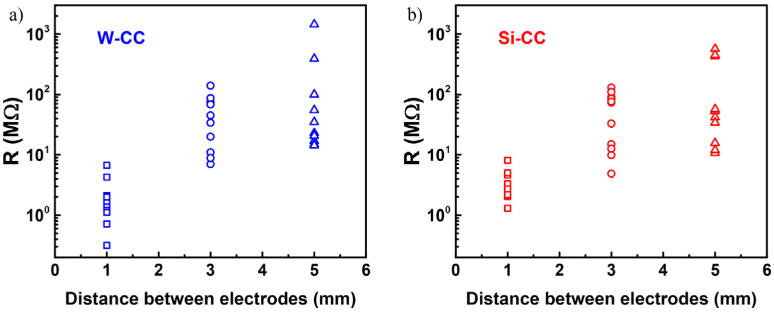

Fig. 6. Electrical resistance of individual glass fibers as a function of the distance between electrodes. (a) W-CC fibers, (b) Si-CC fibers.

somewhat similar to that of W-CC, suggesting as well that a homogeneous distribution of MWCNTs on the fiber is achieved only when the fiber coating is maintained. Thus, the Raman analysis agrees with the SEM observations providing an excellent tool to map the MWCNT spatial distribution onto glass fibers at a larger scale.

3.2. Fiber Surface Roughness

The surface morphology of the glass fibers with and without deposited MWCNTs obtained by AFM is shown in Figure 5. The surface of the glass fibers without (CR) and with coating (CC) prior MWCNTs deposition is shown in Figures 5a and b, respectively. Likewise, Figures 5c–d show the surface of the glass fibers with deposited MWCNTs using either water or a hydrolyzed silane as suspending fluid (see Table 1). The resulting RMS roughness and its CV calculated from the AFM images are summarized in Table 2. The CV can be interpreted as indicative of the homogeneity of the MWCNT deposition onto the fiber surface.

A relative smooth surface can be observed for CC fibers (Figure 5b) while a slightly rougher surface is observed for CR fibers (Figure 5a) which may be due to the removal of the fiber coating. This trend is captured by an RMS surface roughness of 2.07 and 4.05 nm for CC and CR fibers, respectively. Upon MWCNT deposition onto glass fibers, a large increase in the glass fiber roughness is evident. As seen from Figure 5c, when water is used as suspending fluid to deposit MWCNTs onto glass fibers whose coating was removed, a poor deposition with MWCNT agglomerates is observed. On the other hand, using an identical procedure but maintaining the proprietary coating of the glass fibers (Figure 5d) yields a higher density of MWCNTs better dispersed onto the fiber surface, concomitant with the high RMS roughness (26.7 nm) and low CV (0.23). A similar situation is observed when a hydrolyzed silane is used as suspending fluid to deposit MWCNTs onto glass fibers (Figures 5e and f), i.e., a higher density of MWCNTs (higher roughness) with a more homogeneous distribution (lower CV) is observed when the fibers maintain their proprietary coating. The observed increase in fiber roughness upon MWCNT deposition is expected to promote mechanical interlocking/friction between the glass fiber and vinyl ester matrix, which may yield an enhanced interfacial strength for the hierarchical composites.

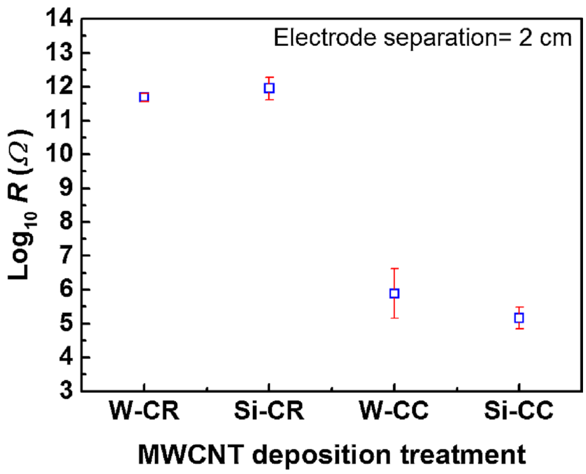

Fig. 7. Electrical resistance of glass fiber tows containing MWCNTs.

3.3. Electrical Resistance of Individual Fibers and Fiber Tows

The as-received E-glass fibers are electrical insulators with volume resistivity in the order of ≈10^{25} Ωcm.[17] A key challenge for the potential use of such glass fibers with deposited MWCNTs for damage sensing in composites through their electrical resistance is that the MWCNTs form an interconnected network on the fiber surface, rendering electrically conductive fibers. Figure 6 presents electrical resistance (R) measurements of the individual glass fibers investigated in this work as a function of the distance between electrodes.

The electrical resistance of fibers whose coating was removed (W-CR and Si-CR) was higher than the reliable detection limit of the 6517B Keithley electrometer (1×10^{16} Ω) and hence they are not reported. On the other hand, for as-received glass fibers (CC) the electrical resistance upon MWCNT deposition is in the order of 1–10^3 MΩ, as seen in Figure 6. Using dip-coating deposition, Zhang et al.[9] also achieved electrical resistances in the order of 10^{-1}–10^3 MΩ upon MWCNT deposition for 1 mm long glass fibers. For W-CC fibers, Figure 6a, the lowest measured electrical resistance is ≈300 kΩ and occurred for an electrode separation (considered as the effective specimen length) of 1 mm. When the electrodes are 3 mm apart, the electrical resistance increases to ≈10–10^2 MΩ. For samples with 5 mm electrode separation, the electrical resistance was in the order of ≈1–10^3 MΩ. For Si-CC fibers, Figure 6b, the lowest electrical resistance was ≈1 MΩ for 1 mm electrode separation and the highest was ≈10^3 MΩ when the electrode are 5 mm apart, showing similar values of R between W-CC and Si-CC. In order to investigate a more realistic composite scenario, the electrical resistance of tows of glass fibers (≈4 000 filaments) containing MWCNTs was also characterized and the results are shown in Figure 7.

For the case of fiber tows, all the experimental conditions used (CC and CR) yield R <TΩ and thus fell within the

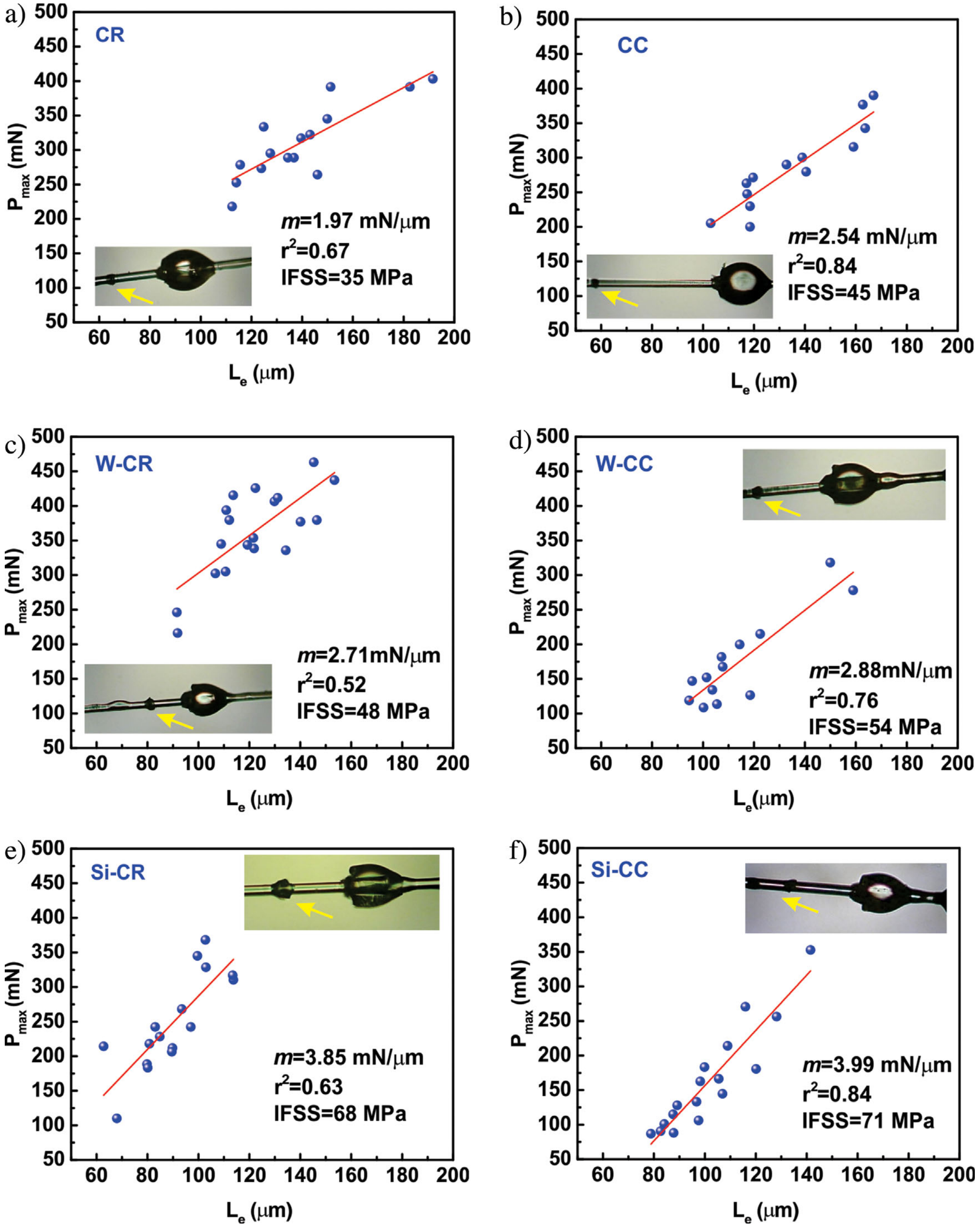

Fig. 8. IFSS between glass fibers and VE resin. (a) CR/VE, (b) CC/VE, (c) W-CR/VE, (d) W-CC/VE, (e) Si-CR/VE, and (f) Si-CC/VE.

operational range of the measuring instrument. Figure 7 shows that the electrical resistance of 2 cm long tows of W-CR and Si-CR fibers are in the order of TΩ. The lower value of R for CR fiber tows with respect to individual CR fibers (Figure 6) can be attributed to the formation of additional conductive paths due to lateral contact among the fibers within the tow. For tows of W-CC and Si-CC fibers, the electrical resistance was ≈300–700 kΩ cm^{-1}, suggesting that these modified fibers can be exploited to manufacture electroconductive composites with multifunctional, strain and damage sensing applications, see ref.[6a,d,9]

3.4. Interfacial Shear Strength between Glass Fibers and Vinyl Ester Resin

In order to assess the role of the deposited MWCNTs onto the glass fibers on the interfacial adhesion between such fibers and a vinyl ester resin, microbond testing was conducted and the results are show in Figure 8. Representative optical images of the debonded resin droplet over a fiber are included as insets in Figure 8. Upon debonding, it is common to observe a cone of matrix left behind at the initial position of the droplet on the fiber. This could be attributed to tensile stresses which induce fracture of the matrix followed by interfacial failure.[18] Unavoidable evaporation of the styrene in the resin droplet during curing can also reduce the mechanical properties of the resin, and hence affect the fiber/matrix interfacial strength.[19]

In Figure 8, the deboning force ($P_{\max}$) is plotted as a function of the embedded drop length (L_e) for all the investigated fiber treatments, and the slope of the linear fitting (m) was employed to calculate the IFSS using Equation 1. The resulting IFSS between the fibers and the vinyl ester resin is listed within the figure along with the slope (m) and the coefficient of determination (r^2).

In spite of the relatively large dispersion inherent to the technique, the trend is clearly visible. The IFSS of CR fibers/VE (35 MPa, Figure 8a) is lower than that of the CC/VE (45 MPa, Figure 8b), since CC fibers contain a coating that is compatible with the vinyl ester resin. These values agree with values reported by other authors.[19,20] When MWCNTs are deposited onto the glass fibers using water, both W-CR/VE (Figure 8c) and W-CC/VE (Figure 8d) show IFSS ≈50 MPa, rendering larger data scattering when the fiber coating is removed. This scattering of the IFFS for W-CR/VE is attributed to the non-homogeneous distribution of MWCNTs onto such fibers, as has been pointed out earlier for fibers whose coating was removed. It is evident that the presence of MWCNTs onto the glass fibers improve the mechanical/interfacial interlocking between the glass fibers and the vinyl ester resin. For W-CR/VE, an increase in the IFSS of ≈37% with respect to that of CR/VE is observed; for W-CC/VE the increase on the IFSS is ≈13% with respect to that of CC/VE. In spite of the scattered data, when silane is used as the suspending fluid for the deposition of MWCNTs, the resulting Si-CR/VE (Figure 8e) and Si-CC/VE (Figure 8f) composites showed an increase in IFSS of ≈40% with respect to their counterparts where only water was used (W-CR/VE and W-CC/VE). This increase in IFSS is attributed to the silane coupling agent (MPS) which is compatible with both, the vinyl ester resin[21] and the MWCNTs,[14] as well to the increased fiber surface roughness due to the presence of MWCNTs, as detected by AFM. The highest IFSS of the glass fiber/MWCNT/vinyl ester system (≈70 MPa) is achieved by depositing MWCNTs onto fibers using a hydrolyzed silane as suspending fluid, either using as-received glass fibers or after removing their fiber coating. Organosilanes have extensively been used in fiber reinforced polymer composites given their ability to form chemical bonds between organic and inorganic materials.[19] For ternary hierarchical composites (micron-size fiber/MWCNTs/polymer), the improved IFSS can be attributed to an increased surface area of interaction between the MWCNT-modified glass fibers and the vinyl ester matrix, increased mechanical interlocking due to the increased fiber roughness upon MWCNT deposition,[12] and to the use of an adequate silane coupling agent which improves the wettability and chemical interactions between the fibers and matrix.[7,12a]

4. Conclusions

Acid oxidized multiwall carbon nanotubes (MWCNTs) were deposited onto as-received glass fibers and onto fibers whose coating (“sizing”) was removed using water and a hydrolyzed silane (3-(trimethoxysilyl) propyl methacrylate, MPS) as suspending fluids. Homogeneous coverage with relative high density of MWCNTs onto the fibers were observed only when the fiber coating was maintained, suggesting a paramount role of the fiber coating in the deposition of MWCNTs. When the fiber coating was removed, aggregates of MWCNTs were observed onto the glass fibers and the deposition was non-homogeneous. The high density of MWCNTs on the fibers and their homogenous distribution rendered an electrical resistance of glass fiber tows in the order of ≈500 kΩ cm^{-1}. The root mean square surface roughness of the as-received glass fibers was ≈2.07 nm^{-1} and increased to ≈27 nm after the deposition of MWCNTs onto their surface using water as suspending fluid, and to ≈18 nm when the silane was used. However, when the fiber coating is removed, the increase in surface roughness of the glass fibers upon MWCNTs deposition is limited. Microbond tests between individual glass fibers containing MWCNTs and a drop of vinyl ester resin showed that the highest improvement in interfacial shear strength (IFSS) was obtained by using a hydrolyzed silane as suspending fluid either using as received glass fibers or using the fibers whose coating was removed. The use of the hydrolyzed silane during the deposition of MWCNTs onto the fibers improved the IFSS between the glass fibers containing MWCNTs and the vinyl ester. The use of a compatible silane as deposition fluid is an adequate alternative for the MWCNT distribution and electrical properties of the resulting fibers but simple distilled water as suspending fluid may suffice to this aim. The role of the silane, however, is more prominent as a coupling agent at the interface formed between the fiber/nanotube and the polymer matrix, improving the interfacial shear strength. The improved electrical and mechanical properties of fibers containing MWCNTs deposited onto their surface can be exploited to manufacture multiscale hierarchical composites with improved multifunctional properties.

Article first published online: November 19, 2015
Manuscript Revised: October 28, 2015
Manuscript Received: July 27, 2015

---

[1] a) J. P. Salvetat, J. M. Bonard, N. H. Thomson, A. J. Kulik, L. Forró, W. Benoit, L. Zuppiroli, *Appl. Phys. A Mater.* **1999**, *69*, 255. b) M. M. J Treacy, T. W. Ebbesen, J. M. Gibson, *Nature* **1996**, *381*, 678.

[2] T. W. Ebbesen, H. J. Lezec, H. Hiura, J. W. Bennett, H. F. Ghaemi, T. Thio, *Nature* **1996**, *382*, 54.

[3] a) E. Pop, D. Mann, Q. Wang, K. Goodson, H. Dai, *Nano Lett.* **2006**, *6*, 96. b) R. S. Ruoff, D. C. Lorents, *Carbon* **1995**, *33*, 925.

[4] J. N. Coleman, U. Khan, W. J. Blau, *Y. K. Gun'ko, Carbon* **2006**, *44*, 1624.

[5] G. Pandey, E. T. Thostenson, *Polym. Rev.* **2012**, *52*, 355.

[6] a) S.-l. Gao, R.-C. Zhuang, J. Zhang, J.-W. Liu, E. Mäder, *Adv. Funct. Mater.* **2010**, *20*, 1885. b) A. Godara, L. Mezzo, F. Luizi, A. Warrier, S. V. Lomov, A. W. van Vuure, L. Gorbatikh, P. Moldenaers, I. Verpoest, *Carbon* **2009**, *47*, 2914. c) L. Tzounis, M. Kirsten, F. Simon, E. Mäder, M. Stamm, *Carbon* **2014**, *73*, 310. d) J. Zhang, J. Liu, R. Zhuang, E. Mäder, G. Heinrich, S. Gao, *Adv. Mater.* **2011**, *23*, 3392.

[7] A. Warrier, A. Godara, O. Rochez, L. Mezzo, F. Luizi, L. Gorbatikh, S. V. Lomov, A. W. VanVuure, I. Verpoest, *Compos. Part A Appl. S*. **2010**, *41*, 532.

[8] a) P. Lv, Y.-Y. Feng, P. Zhang, H.-M. Chen, N. Zhao, W. Feng, *Carbon* **2011**, *49*, 4665. b) H. Qian, A. Bismarck, E. S. Greenhalgh, G. Kalinka, M. S. P. Shaffer, *Chem. Mater.* **2008**, *20*, 1862. c) S. S. Wicks, R. G. de Villoria, B. L. Wardle, *Compos. Sci. Technol*. **2010**, *70*, 20.

[9] J. Zhang, R. Zhuang, J. Liu, E. Mäder, G. Heinrich, S. Gao, *Carbon* **2010**, *48*, 2273.

[10] a) Q. An, A. N. Rider, E. T. Thostenson, *ACS Appl. Mater. Interfaces* **2013**, *5*, 2022. b) J. Guo, C. Lu, *Carbon* **2012**, *50*, 3101. c) J. D. Schaefer, A. J. Rodriguez, M. E. Guzman, C.-S. Lim, B. Minaie, *Carbon* **2011**, *49*, 2750.

[11] Q. Zhang, J. Liu, R. Sager, L. Dai, J. Baur, *Compos. Sci. Technol*. **2009**, *69*, 594.

[12] a) M. Li, Y. Gu, Y. Liu, Y. Li, Z. Zhang, *Carbon* **2013**, *52*, 109. b) M. Zu, Q. Li, Y. Zhu, M. Dey, G. Wang, W. Lu, J. M. Deitzel, J. W. Gillespie Jr, J.-H. Byun, T.-W. Chou, *Carbon* **2012**, *50*, 1271.

[13] F. Avilés, J. V. Cauich-Rodríguez, L. Moo-Tah, A. May-Pat, R. Vargas-Coronado, *Carbon* **2009**, *47*, 2970.

[14] F. Avilés, C. A. Sierra-Chi, A. Nistal, A. May-Pat, F. Rubio, J. Rubio, *Carbon* **2013**, *57*, 520.

[15] J. J. Ku-Herrera, F. Avilés, A. Nistal, J. V. Cauich-Rodríguez, F. Rubio, J. Rubio, P. Bartolo-Pérez, *Appl. Surf. Sci*. **2015**, *330*, 383.

[16] B. Miller, P. Muri, L. Rebenfeld, *Compos. Sci. Technol*. **1987**, *28*, 17.

[17] F. T. Wallenberger, in *Fiberglass and Glass Technology: Energy-Friendly Compositions and Applications*, (Eds: F. T. Wallenberger, P. A. Bingham), Springer, New York **2010**.

[18] P. J. Herrera-Franco, L. T. Drzal, *Composites* **1992**, *23*, 2.

[19] X. Dirand, B. Hilaire, J. P. Soulier, M. Nardin, *Compos. Sci. Technol*. **1996**, *56*, 533.

[20] T. H. Cheng, F. R. Jones, D. Wang, *Compos. Sci. Technol*. **1993**, *48*, 89.

[21] S. H. Saidpour, M. O. W. Richardson, *Compos. Part A Appl. S* **1997**, *28*, 971.